Poultry Science®

A network pharmacology and transcriptome analysis of the therapeutic effects of tea tree oil on the lungs of chicks exposed to hydrogen sulfide

Yachao Wang,[*,†,1,2] Yilei Liang,[*,†,1] Li Jiang,[*] Xuegang Luo,[*,†] Tingting Cheng,[*,†] and Xiaoyan Long[*,†]

[*]*School of Life Science and Engineering, Southwest University of Science and Technology, Mianyang, Sichuan 621000, China; and* [†]*Biomass Center, School of Life Science and Engineering, Southwest University of Science and Technology, Mianyang, Sichuan 621000, China*

ABSTRACT This study investigated the use of tea tree oil (**TTO**) in the treatment of H_2S-induced lung injury in chickens, focusing on the detoxification mechanism. H_2S can damage the respiratory system and reduce growth performance. TTO can improve immune inflammation and growth performance. The mechanism by which TTO mitigates the harmful effects of H_2S on chicken lungs remains unclear. Therefore, the experimental model was established by H_2S exposure and TTO addition in drinking water. The 240 one-day-old Roman pink chicks were selected for the experiment. The trial was divided into control group (**CON**), treatment group (**TTG**, 0.02 mL/L TTO+H_2S) and H_2S exposure group (**AVG, H_2S**). There were 4 replicates in each group and the trial lasted for 42 d. The therapeutic effect of TTO on lung injury in chickens were determined by growth performance evaluation, transcription sequencing and network pharmacology analysis. The results showed that in the test's third week, the body weights of the chickens in the CON were higher than those in the AVG and TTG ($P < 0.05$). Pathological sections showed that TTO alleviated the symptoms of lung inflammation and bleeding caused by ROS. As showed by transcriptional sequencing, the mRNA expression of apoptosis-related genes Caspase-9, BAK-1, BCL-2 and BAX were significantly altered ($P < 0.05$). Meanwhile, the mRNA expression of inflammation-related genes IL-2, IL-6, and IL-17 were downregulated ($P < 0.05$). Network pharmacological analysis showed that CA2, CA4, GABRA5 and ADH1C were the key targets of TTO. The TTO treatment significantly altered these targets ($P < 0.05$). Molecular docking confirmed the strong binding ability between the active component and the targets. This study showed that TTO inhibits H_2S-induced oxidative damage to the lungs, thereby improving their health status. This provides a new solution for the prevention of harmful gas in the poultry industry.

Key words: H_2S, tea tree oil, apoptosis, lung, network pharmacology

2024 Poultry Science 103:104180
https://doi.org/10.1016/j.psj.2024.104180

INTRODUCTION

Hydrogen sulfide (**H_2S**) is the main harmful gas pollutant in livestock and poultry houses (Song et al., 2021). Hydrogen sulfide from the decomposition of feed and manure during feeding poses a potential risk to humans and animals (Huang et al., 2019). Inhaled H_2S entered the blood circulation through the respiratory system and affected tissues and organs throughout the body (Guo et al., 2019). Once the concentration of H_2S in the bred environment is too high, it will cause serious damaged to the respiratory system of chickens (Li et al., 2020). Chen et al. (2019) found that H_2S exposure led to the activation of FOS/IL8 pathway in the trachea of chickens, resulting in an increase in MDA and H_2O_2 content, and a decreased in the content of superoxide dismutase (**SOD**), catalase (**CAT**) and glutathione (**GSH**) antioxidant substances. In addition, H_2S also damages the chickens immune system, led to increased expression of tumor necrosis factor-α (**TNF-α**), interleukin-6 (**IL-6**) and interferon-γ (**IFN-γ**) and aggravates the inflammatory response of chickens (Hu et al., 2018). Meanwhile, H_2S could activate the expression of Caspase-3 and Caspase-9 proteins and induce apoptosis of immune organs and respiratory system (Hu et al.,

Received June 10, 2024.
Accepted August 1, 2024.

[1]These authors are common first authors.

[2]Corresponding author: wangyachao@swust.edu.cn

2018; Liang et al. 2024). Even H_2S exposure could lead to asphyxiating death and decreased production performance in chickens (Guo et al., 2019). Therefore, antibiotics are often used to treat H_2S-induced damage in livestock and poultry breeding. However, overuse of antibiotics has led to a dramatic increase in drug-resistant bacteria, posed a serious threat to public health safety (Cully Megan, 2014). Therefore, in this context, the use of Chinese herbs to replaced various chemical drugs has become a new scheme, included herbal medicines (Huang et al., 2021) and plant extracts (Khalaji et al., 2012).

Tea tree oil (**TTO**), as a natural vegetable oil, has a unique fragrance and its main components included Terpinen-4-ol, 1, 8-lentol and α-pinecinol (Bekhof et al., 2023). TTO has been shown to have anti-inflammatory (Liang et al., 2024) and antioxidant (Liu et al., 2022) effects. In addition, TTO is considered as an effective alternative to antibiotics due to it is easy extraction and absence of residues (Bo et al., 2023). It is reported that added TTO to daily feed could not only improved growth performance but also increased SOD and CAT content (Yang et al., 2022). Liang et al. (2024) found that adding TTO to drinking water could alleviate the oxidative stress caused by H_2S through the CYP450s/ reactive oxygen species (**ROS**) pathway and increase the content of CAT and SOD. At the same time, the study also found that added TTO to drinking water could reduce the inhibitory effect of H_2S on the body weight of chickens and improved the growth performance of chickens (Liang et al., 2024). These positive effects were mainly attributed to the excellent performance of TTO in improved nutrient utilization, enhancing antioxidant capacity and improved microbial community structure (Liu et al., 2022; Liu et al., 2023a; Liu et al., 2023b;). In addition, the study found that the addition of TTO in drinking water could reduce the mRNA expression levels of inflammatory factors TNF-α, interleukin-4 (**IL-4**) and IFN-γ, thus improved the immunity of chickens (Liang et al., 2024). Relevant studies have also found that adding TTO to chicken diets can not only increased chicken body weight and averaged daily gain, but also regulated the levels of immune factors IFN-γ, TNF-α and interleukin-2 (**IL-2**) (Liu et al., 2023b). In addition, studies have shown that added TTO to feed can effectively treat diseases such as bronchitis and bronchitis (Tian and Piao, 2019).

The main objective of this study was to investigate the effects of TTO supplementation in drinking water on growth performance and lung injury in H_2S-exposed chickens, focusing on the detoxification mechanism. Therefore, in this study, transcriptomics, network pharmacology and molecular docking were used to analyze and screen the key targets and detoxification mechanisms of TTO in alleviating H_2S-induced growth performance and lung injury in chickens. It is expected to further the mechanism of action of hydrogen sulfide exposure to TTO ease poultry research provides new ideas and new methods.

MATERIALS AND METHODS

Reagents

Hematoxylin, eosin, hydrochloric acid, xylene, absolute ethanol, and 4% paraformaldehyde were purchased from Chengdu Cologne Chemicals Co., Ltd., Chengdu, China. Resin glue was purchased from Nanchang Yulu Experimental Equipment Co., Ltd., Nanchang, China. Annexin V-FITC apoptosis detection kit, propidium iodide (**PI**) staining solution, mitochondrial membrane potential kit and trizol reagent was purchased from Nanjing Jiancheng Biotechnology Co., Ltd. (Nanjing, China). VAHTS Universal V5 RNA-seq Library Prep was from Solebo Biotech (Beijing, China). TTO was supplied by Jiangsu Wuxi Chenfang Biotechnology Co., Ltd., Wuxi, China (Annex 1). The main components of TTO were Terpinen-4-ol and γ-Terpinene, accounting for 50.31% and 20.06%. Roman pink chicks were purchased from the Sichuan Tieqilishi Food Co., Ltd. (Mianyang, China). H_2S was purchased from Zibo Dijia Special Gas Co., Ltd. (Zibo, China). Hydrogen sulfide detection instrument Shenzhen Yifan Environment Co., Ltd. (YF-8801-OU, Shenzhen, China).

Experimental Animals and Experimental Design

A total of 240 one-day-old Roman pink chicks of similar body size and condition were selected. Chicks were randomly divided into 3 treatment groups with 4 replicates per group and 20 chicks per replicate. The chicks were kept in 3 separate environmental control boxes. Exposure tests were performed using external H_2S and H_2S concentration was measured using a H_2S detector. The H_2S concentration was controlled according to the experimental design requirements of Song et al. (2021). The TTO concentration in drinking water was set according to the experiment of Liang et al. (2024). Control group (**CON**) chicks did not receive any treatment. H_2S exposed Group (**AVG**) chicks were raised in an environmental control tank containing H_2S. Chicks in the TTO treatment group (**TTG**) were fed in an environmental control tank containing H_2S and 0.02 mL/L TTO was added to drinking water. The specific experimental design is shown in Table 1. The test period was 42 d. The 3 groups of temperature, humidity and light

Table 1. Experimental design.

Stage	Groups	H_2S concentrationn (mg/m^3)
1-21 d	Normal group (CON)	$H_2S \leq 0.5$(safety range)
	H_2S exposure group (AVG)	$3.5 \leq H_2S \leq 4.5$
	TTO treatment group (TTG)	$3.5 \leq H_2S \leq 4.5$, 0.02 ml/L TTOl was added to drinking water
22-42 d	Normal group (CON)	$H_2S \leq 0.5$
	H_2S exposure group (AVG)	$19.5 \leq H_2S \leq 20.5$
	TTO treatment group (TTG)	$19.5 \leq H_2S \leq 20.5$, 0.02 ml/L TTO was added to drinking water

time were relatively consistent during the whole test. Roman pink chicks can freely drink water and eat a basic diet (Liu et al., 2023b) (Annex 2). After 42 d, all the chickens were sacrificed by anesthesia, and a 2.0 cm × 2.0 cm × 0.3 cm sample was removed from the left upper lobe lung. The sample was preserved in 4% paraformaldehyde for 24 h, and then pathological observations of the lung tissue slices were conducted. Excess tissue was stored at −80°C for future use.

Determination of the Growth Performance of the Chickens

The initial body weight of each chick was measured before the experiment. The chickens' weight and feed consumption were measured once a week at 6:00 to 7:00 am during the trial. Each measurement was taken out of the chickens before feeding. The average daily feed intake (**ADFI**), average daily gain (**ADG**), feed to gain (**F**/**G**) ratio, and mortality (Szymański et al., 2020) of the chickens were calculated 42 d after the end of the experiment. The formulae used for these computations are as follows (Ruan et al., 2023):

ADFI = total phase feed intake (g)/number of days (d).
ADG = stage weight gain (g)/feeding days (d).
F/G ratio = total feed consumed (g)/weight gain (g).
Mortality (%) = number of dead chickens/total number of chickens.

Analysis of Tissue Sections

The tissue samples fixed with 4% paraformaldehyde for 24 h were removed, rinsed with running water for 30 min, trimmed, put into pathological embedding basket, and then dehydrated with 75, 85, 95%, and 100% alcohol for 6, 10, 4 and 2 h, respectively. At the end of dehydration, the lung tissue was placed into xylene for transparency twice for 15 min each. The clear tissues were removed and immersed in wax for 3 h before embedding in paraffin. The tissues were then cut into 5 μm thick slices using a microtome (Leica Biosystems Nussloch GmbH, RM2235, Nussloch, Germany), flattened and fished on slides in warm water, and then baked at 60°C for at least 2 h. The slices were then deparaffinized with xylene, washed with running water for 20 min, stained with hematoxylin for 30 min, washed with running water for 20 min, differentiated with hydrochloric acid alcohol, stained with eosin for 5 min, and finally dehydrated with gradient alcohol, transparent with xylene, and sealed with resin glue. The histopathological changes were observed under an electron microscope (TE2000-S, Nikon Corporation, Tokyo, Japan) and the whole tissue was completely scanned. Both normal tissues and parts with obvious lesions were photographed and recorded by the microscopic imaging system, and the histological damage of each sample was described and scored (Appendix 3) (Ortega et al., 2018).

Flow Cytometry Technology to Detect Reactive Oxygen Species, Membrane Potential, and Apoptosis

The lung tissue was cut mechanically, filtered through a 300-mesh filter cloth, and centrifuged at 3,000 g for 5 min. The cell concentration was then adjusted to 10^6 cells/mL with phosphate buffer solution (**PBS**). Subsequently, the cells were incubated at 37°C for 20 min. The fluorescence intensity of the cells was measured when the emission wave was 530 nm (Lyublinskaya et al., 2017). CytExpert flow cytometry (Thermo Fisher Technologies, CytExpert, Waltham, MA) was used and ROS data were analyzed using Kaluza 2.1 software.

To adopt the mitochondrial membrane potential kit membrane potential, adding a suitable amount of mitochondrial membrane potential dyes, the cells were incubated in an incubator at 37°C for 15 min for dyeing. Incubation at 37°C was followed by centrifugation at 400 g (4°C, 4 min). The discarded supernatant was removed and washed twice with 1×PBS and centrifuged again (400g, 4°C, 4min). Finally, 100 μL of the cell suspension was transferred to a flow tube and analyzed by fluorescence spectrophotometer (Ikeda Ya (Shenzhen) Industrial Co., LTD., SH-1000, Shenzhen, China)or flow cytometry (Thermo Fisher Technologies, CytExpert, Waltham, MA) (green fluorescence: Ex/Em = 510/527 nm; red fluorescence: Ex/Em = 585/590nm) to observe the membrane potential (Liu et al., 2019; Brings et al., 2022).

Lung cell apoptosis was determined using a detection kit. Firstly, the lung cell concentration was adjusted with PBS to 1 × 10^6 cells/ml. Subsequently, 5 μL of Annexin V-FITC staining fluorescent dye (Nanjing Jiancheng Bioengineering Institute) and PI (Nanjing Jiancheng Bioengineering Institute) were added for staining. Apoptosis was analyzed by flow cytometry immediately after incubation with light at 26°C for 15 min (Groß et al., 2024).

Transcription Sequencing

The collected control samples and treated lung samples were subjected to transcriptome sequencing. Total RNA was extracted using TRIzol reagent according to the manufacturer's instructions in triplicate for each sample. RNA purity and quantification were identified using a NanoDrop 2000 spectrophotometer (Thermo Scientific). RNA integrity was assessed using an Agilent 2100 Bioanalyzer (Agilent Technologies, Santa Clara, CA). Transcriptome libraries were constructed using the VAHTS Universal V5 RNA-seq Library Prep kit according to the manufacturer's instructions. Transcriptome sequencing and analysis were performed by Shanghai Ouyi Biotechnology Co., Ltd. Shanghai, China. Using edgeR and the CON group and DESeq2 software to analyze differentially expressed. Sequence quality was first assessed using Fastp to determine the quality of the raw reads. Then, genes with $P < 0.05$ and a fold change (FC)

>1.5 times were selected as differential genes. Subsequently, bioinformatics software (https://cloud.oebiotech.cn) was used to map volcanic maps and heat maps.

Features Enrichment and Protein-Protein Interaction Analysis

Bioinformatics software enrichment of gene ontology (**GO**) (https://cloud.oebiotech.cn), which is based on path analysis (**KEGG**), was used to identify differentially expressed genes (**DEGs**) and their main biological functions (Li et al., 2021). Genetic variations were imported to the STRING database (https://string-db.org/), the medium confidence interval was set to 0.4, and free nodes were hidden. The output was in TSV format file, and the generated TSV file was input into Cytoscape 3.8.2 software to remove the single non-interacting protein. A Network Analyzer plug-in was used for topological analysis, and the PPI network was constructed according to the degree value to obtain key target proteins.

Screening and Target Prediction of Active Components of TTO

Using the Traditional Chinese Medicine Systems Pharmacology Database and Analysis Platform (**TCMSP**, http://tcmspw.com/tcmsp.php) to determine the active ingredients in TTO. The targets of nine TTO components were obtained from the UniProt database (http:/www.uniprot.org/). Venny 2.1.0 software (https://bioinfogp.cnb.csic.es/tools/venny), which targets differences in the ingredients gene targets in intersection, which is a potential target of TTO treatment.

Molecular Docking

From the PubChem database (https://PubChem.Ncbi.WhileNLM.Nih.Gov/) for compound structure. Protein structures were obtained from the PDB database (https://www.rcsb.org/). Autodock Vina software was used for molecular docking, and Discovery Studio software was used to optimize the docking results output.

Real-Time Fluorescent PCR

Total RNA from lung tissue was extracted using an RNA extraction kit, and a biological analyzer was used to assess the quality and content of the RNA. Subsequently, total RNA was reverse transcribed into cDNA using a cDNA synthesis system (Invitrogen, Carlsbad, CA). The expression of IL-2, IL-6, interleukin-17 (**IL-17**), BAK-1 (BCL2 antagonist 1), Caspase-9, BCL-2 (BCL2 apoptosis regulator), and BAX genes in the lung was then validated (Appendix 3). Use TB Green Premix Ex Taq II kit (Takara Bio, Japan, Tokyo, Japan) was amplified by PCR on a fluorescent quantitative PCR apparatus (Murray (Shanghai) Biotechnology Co., LTD, Light Cycler 180, Shanghai, China) according to manufacturer's instructions. (Shi et al., 2024; Sun et al., 2024). Primers were designed using Primer Premer5 software. The mRNA expression levels of all genes were normalized to β-actin as an internal reference control gene. The relative gene expression of the samples was calculated using the CT method (Song et al., 2021).

Data Analysis

SPSS22.0(IBM Corp., Armonk, New York, NY) software was used for single-factor analysis to identify significant differences between groups. The experiment was repeated 3 times to take the average value, and the data results were represented by the mean ± standard deviation (M ± SD). The mortality rate of chickens was adjusted using the standardized mortality rate (**SMR**) to obtain the survival rate (Szymański et al., 2020). Graphs were drawn using GraphPad Prism Software 8.0 (GraphPad Software Inc., Chicago, IL). The same letter between the groups indicated no significant difference ($P > 0.05$), and the different letter between the groups indicated significant difference ($P < 0.05$).

RESULTS

Active Ingredients in TTO

The TCMSP database was used to identify the active ingredients in TTO, included Terpinen-4-ol, Limonene, Globulol and Terpinolene, δ-Cadinene, Ledene, γ-Limonene, ρ-Cymene, and α-Terpineol (Annex 5). Figure 1 shows the TTO 9 ingredients in formula.

Improvement of Growth Weight of Chickens by TTO

This experiment design as shown in Figure 2A. Figure 2B shows the changed trend in the body weights of the chickens in the 3 groups each week over the 42-d period. It is important to note that in the third week of the experiment, the chickens' body weights in the CON group were significantly higher than those in the AVG and TTG ($P < 0.05$). The experimental results also showed that the ADG of the chickens increased ($P > 0.05$) and the F/G significantly decreased ($P < 0.05$) after 42 d of the TTO treatment compared with the AVG (Figures 2D and 2E). In addition, the TTO treatment slightly reduced the ADFI and improved survival rate, but not significantly, compared with the AVG ($P > 0.05$) (Figures 2C and 2F). Overall, TTO treatment increased the body weight of chickens compared to AVG.

Transcriptome Analysis

The collected lung tissue samples were subjected to transcription sequenced. The inter-group similarity between the 3 groups of samples were close to 1,

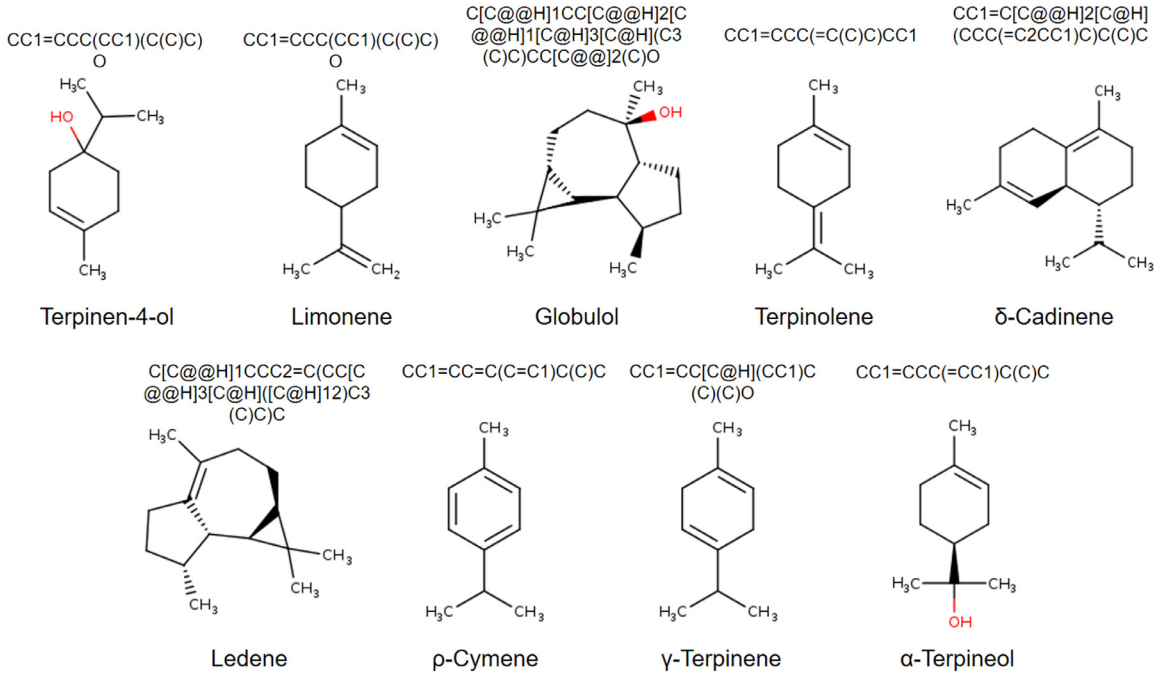

Figure 1. TTO active ingredient.

indicated that the samples were highly similar (Figure 3A). PCA (principal component analysis) revealed significant sample differences between the groups, indicating that the experimental treatment yielded positive results (Figure 3B). The obtained data were subjected to differential analysis, and genes with $P < 0.05$ and a FC > 1.5 were selected as differential genes. Genetic variations were detected in 3,369 genes in the AVG, with 1,694 upregulated genes and 1,675 downregulated genes. In total, 1,950 DEGs were detected in the TTG, including 988 upregulated and 962 downregulated genes (Figure 3B). The Veen analysis of the detected differential genes revealed 89 common differential genes among the 3 groups (Figure 3C).

The GO and KEGG databases were utilized to identify differences in gene function annotation. Genetic variations detected in the AVG was primarily enriched in particular processes, including the immune system process, biological regulation and the response to stimuli. In the cellular component, the differential genes were mainly enriched in the cell part, membrane, membrane part, and other enriched entries. In terms of molecular function, antioxidant activity and enzyme regulator activity were significantly enriched due to oxidative stress (Figure 3D). Cellular processes, cell, binding, biological regulation, cell part and organelle were found to be the main enriched entries in the TTG (Figure 3E). In the AVG, KEGG function enrichment analysis revealed cytokine−cytokine receptor interactions, an intestinal immune network for IgA production and apoptosis and cellular senescence, NOD-like receptor signaling, cytosolic DNA sensing, and P53 signaling pathways. Other pathways associated with immunity and cell death were also enriched in the AVG, indicating that H_2S caused

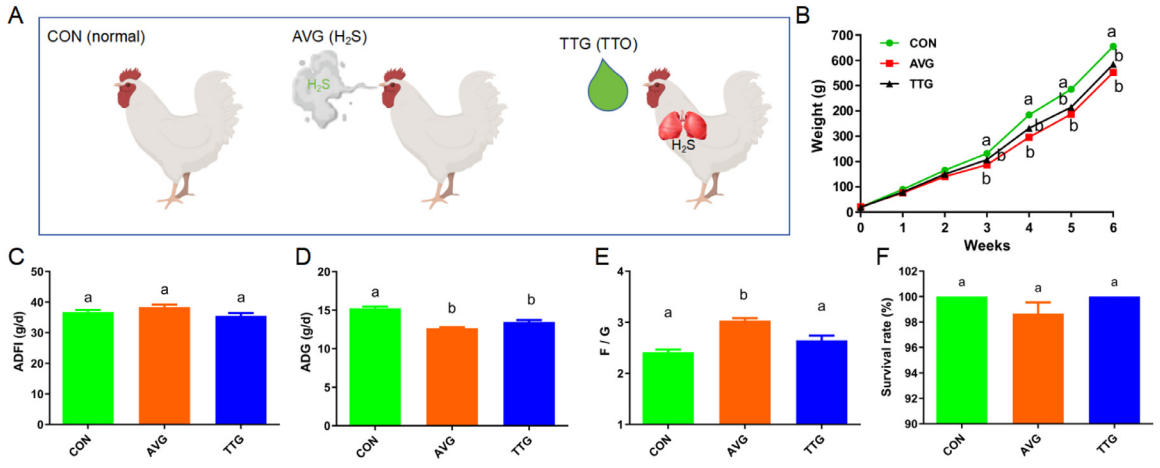

Figure 2. Effect of TTO on the growth performance of the chickens. (A) Experimental design model. (B) Changes in the chickens' body weights during the experiment. (C) ADFI. (D) ADG. (E) F/G. (F) Mortality. CON: control group. AVG: H_2S-exposed group. TTG: TTO treatment group. Different letters between groups indicate significant differences ($P < 0.05$). The data are expressed as mean ± standard deviation (M ± SD).

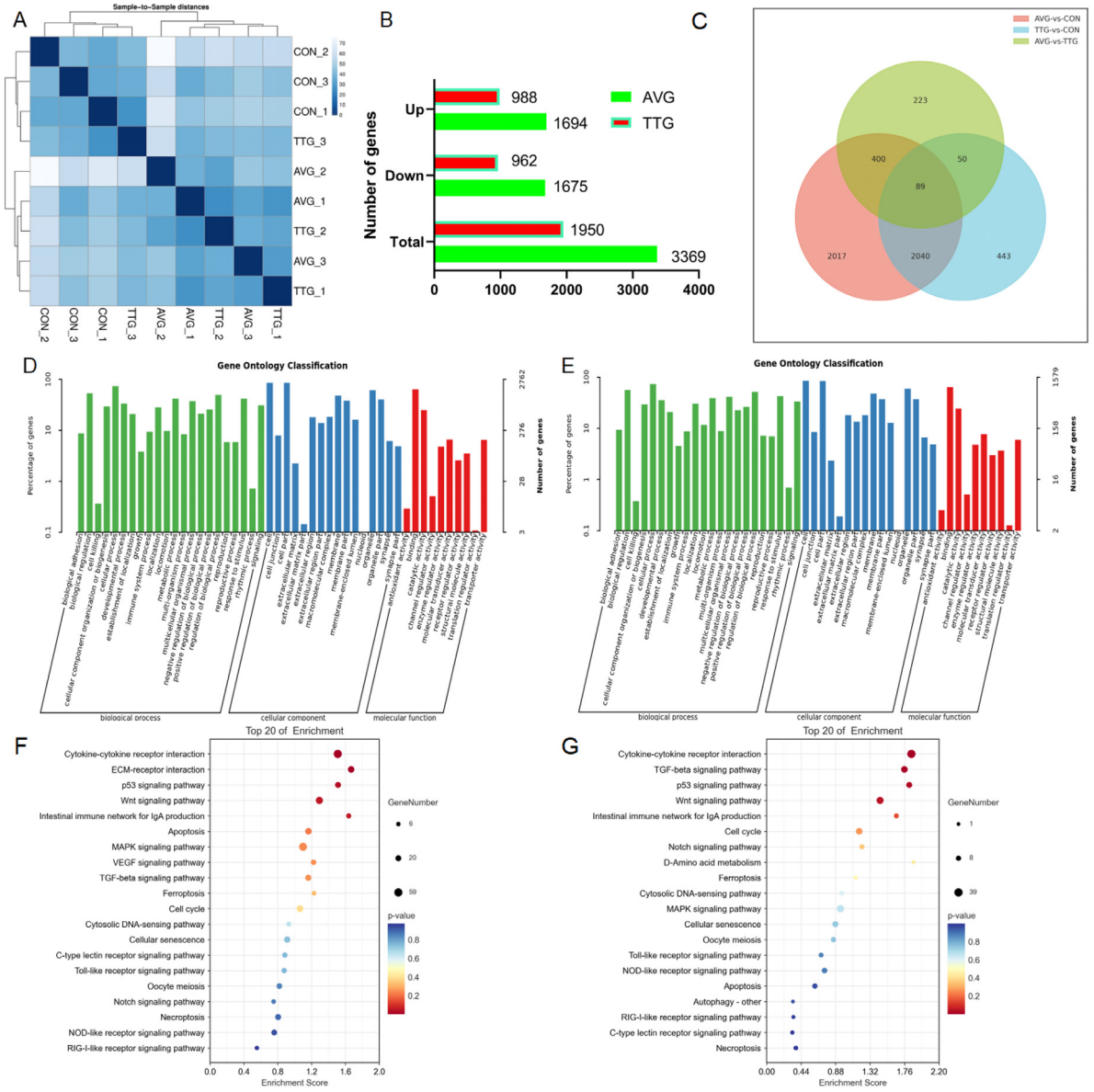

Figure 3. Effect of TTO on transcriptome. (A) Correlation analysis between groups. (B) Number of differential genes. (C) Veen analysis. (D) GO enrichment in the AVG. (E) GO enrichment in the TTG. (F) KEGG enrichment in the AVG. (G) GO enrichment in the TTG.

inflammation and cell death in the lung (Figure 3F). In the TTG, cytokine−cytokine receptor interactions; an intestinal immune network for IgA production and apoptosis; and cellular senescence; NOD-like receptor signaling, cytosolic DNA-sensing, and P53 signaling pathways were significantly enriched (Figure 3G). However, the differential genes in the enrichment pathways were significantly reduced ($P < 0.05$). Thus, the TTO treatment could significantly modulate immunity and lung cell death.

Effects of TTO on Tissue Damage

Microscopic observations revealed varying degrees of pathological damage in lung tissues and organs. These injuries included massive hemorrhage in the lumen of the secondary bronchus, hemorrhage in the pulmonary compartment and dilatation and congestion of the respiratory capillaries. Specifically, the structure of the lung tissues in the CON was normal and no obvious pathological damaged was observed. However, pulmonary hemorrhage, included in the secondary bronchi and pulmonary chambers, and congestion of respiratory capillaries were found in the AVG ($P < 0.05$). In contrast, in the TTG, only minor lung hemorrhage, including secondary bronchi, was observed, with no congestion in the pulmonary chambers or respiratory capillaries ($P < 0.05$) (Figure 4A).

To gain more insight into the effects of TTO on H_2S-induced lung cell damage, flow cytometry was used to detect ROS generation, cell apoptosis, and membrane potential changes. The results of flow cytometry showed that the ROS content in the AVG was significantly higher than that in the other groups ($P < 0.05$), indicating that AVG caused oxidative stress damage. However, following the TTO treatment, the ROS content in the tissues significantly decreased ($P < 0.05$) and returned

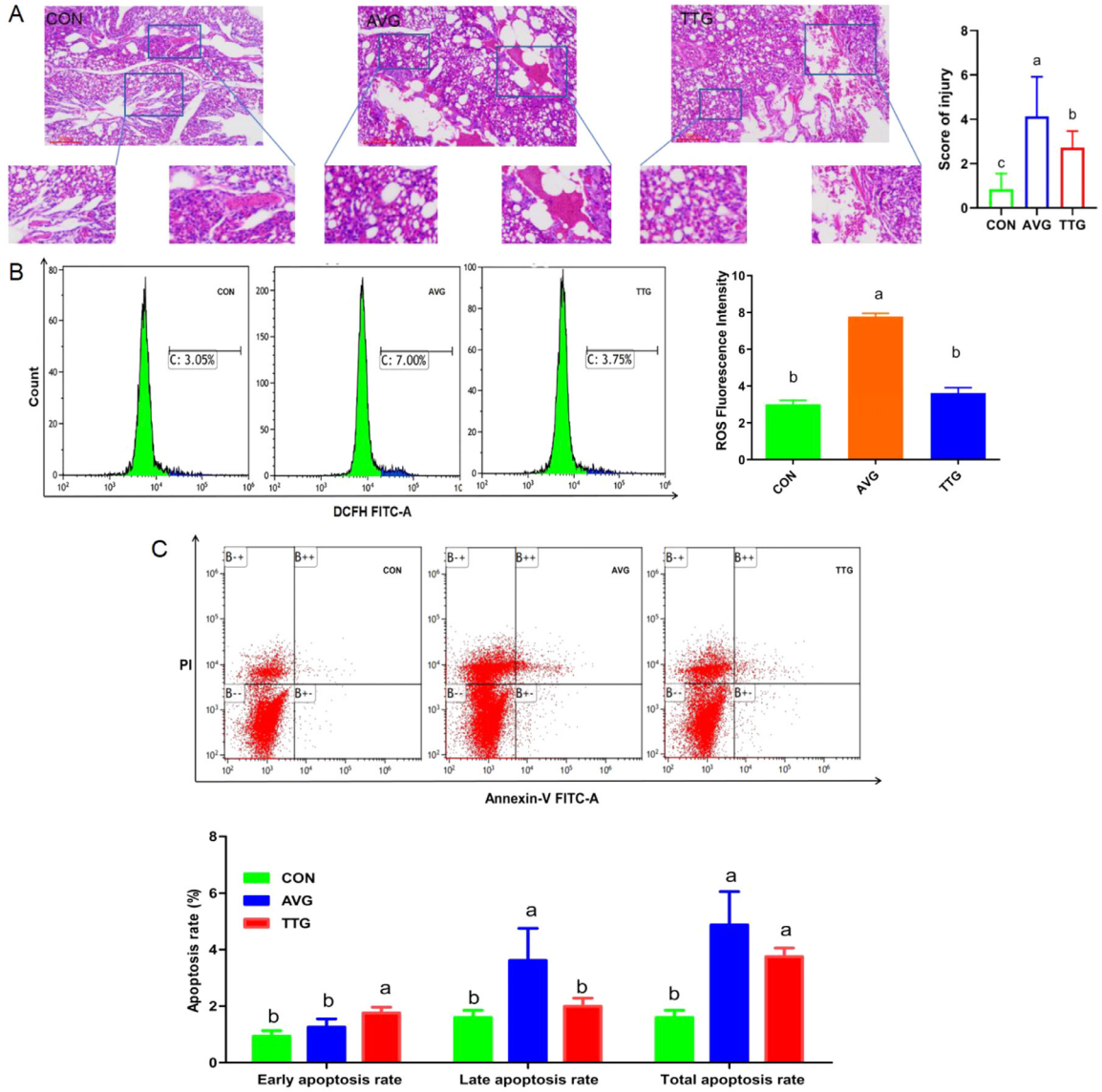

Figure 4. Lung tissue damage. (A) Lung pathological section, HE stained, Bar = 100 μm. (B) ROS flow in lung cells. (C) Apoptosis flow in the lung. CON: control group. AVG: H_2S exposed group. TTG: TTO treatment group. Different letters between the groups indicate significant differences ($P < 0.05$). The data are expressed as mean ± standard deviation (M ± SD).

almost to normal levels ($P > 0.05$) (Figure 4B). Annexin V/PI staining showed that compared with the CON, the late apoptosis rate and total apoptosis rate of lung tissue cells in the AVG were significantly increased ($P < 0.05$). Compared with the CON group, the early apoptosis rate in the TTG was significantly increased ($P < 0.05$), but the total apoptosis rate did not change significantly ($P > 0.05$) (Figure 4C). The results showed that the apoptosis of lung tissue cells in both the AVG and TTG showed an increased trend. Measurement of the membrane potential of chicken lung cells using the JC-1 probe revealed significant depolarization of the mitochondrial membrane potential in the AVG compared with the CON ($P < 0.05$) (Figure 5A). However, the depolarized effect of H_2S on chicken lung cells was significantly reduced in the TTG.

The cluster analysis of DEGs showed that the gene changes between groups were obvious (Figures 5B and 5C). In the apoptotic pathway of cell death in the AVG, 28 apoptotic genes were detected, of which 13 were upregulated and 15 were downregulated (Figure 5D). In the TTG, 8 DEGs were detected, of which 2 were upregulated and 6 were downregulated (Figure 5C). The PPI analysis clearly revealed the interaction between these DEGs (Figures 5E and 5F). The results indicated that the TTO treatment significantly suppressed the expression levels of apoptotic genes ($P < 0.05$). Specifically, the expression levels of BCL2A1 (BCL2 related protein A1), BID (BH3 interacting domain death agonist), Caspesa-8, Caspesa-9, FASLG (Fas ligand), ITPR2 (inositol 1,4,5-trisphosphate receptor type 2) and TNFSF10 (TNF superfamily member 10) were significantly inhibited after the TTO treatment. To verify the accuracy of sequencing, the mRNA expression of the Caspesa-9 gene was examined by qRT-PCR, and the results were consistent with the sequencing results ($P < 0.05$) (Figure 5G). In addition, the apoptosis-related genes BAK-1, BCL-2,

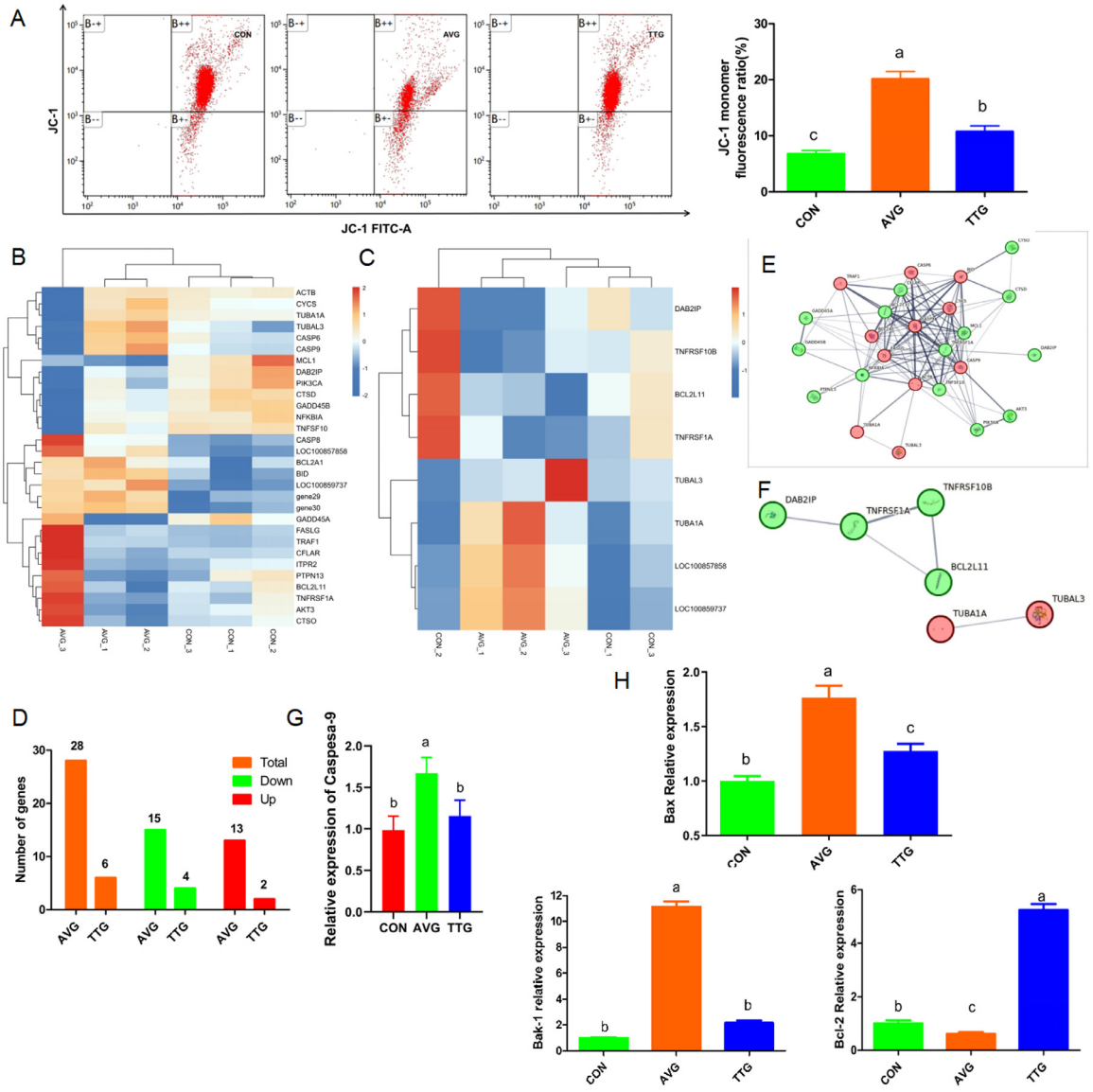

Figure 5. Effect of TTO on cell apoptosis in lung tissue. (A) Membrane potential depolarization assessed by flow cytometry. (B) AVG differential gene cluster heat map. (C) TTG differential gene cluster heat map. (D) Number of DEGs. (E) AVG DEGs in the PPI analysis. (F) TTG DEGs PPI analysis. (G): Caspesa-9 mRNA expression. (H) BAK- 1, BCL-2, and BAX gene mRNA expression. CON: control group. AVG: H_2S-exposed group. TTG: TTO treatment group. Different letters between the groups indicate significant differences ($P < 0.05$). The data are expressed as mean ± standard deviation (M ± SD).

and BAX were detected (Figure 5H). The results showed that H_2S exposure significantly reduced the mRNA expression of the BCL-2 gene ($P < 0.05$) and increased the mRNA expression levels of the apoptotic genes BAK-1 and BAX ($P < 0.05$). However, the TTO treatment significantly reduced the mRNA expression levels of the apoptotic genes BAK-1 and BAX ($P < 0.05$) and increased the mRNA expression level of the anti-apoptotic gene BCL-2 ($P < 0.05$). These results further indicated that TTO had a favorable anti-apoptotic effect.

Effects of TTO on Immune System

In the transcriptome analysis, in total, 49 DEGs related to immunity were detected in the AVG, of which 39 genes were upregulated (Figures 6A and 6C), and 10 genes were downregulated. In the TTG, 19 immune-related genes were differentially expressed, with 16 upregulated and 3 downregulated genes (Figures 6B and 6D). All in all, IL18, IL6, Myd88 (myeloid differentiation primary response gene 88), and NFKBIA (NFKB inhibitor alpha) genes were significantly downregulated. To further understand the interactions between these DEGs, PPI analysis was performed (Figures 6E and 6F).

To verify the accuracy of the transcriptome data, the IL-6 gene was selected for qRT-PCR analysis. The results showed that H_2S exposure caused significant downregulation of the IL-6 gene mRNA expression level ($P < 0.05$). Similarly, in the TTG, the IL-6 gene mRNA expression showed a significant downward trend ($P < 0.05$). This found was consistent with the FC trend of expression in the transcriptome (Figures 6G and 6H). To further explored the effects of TTO on the immune

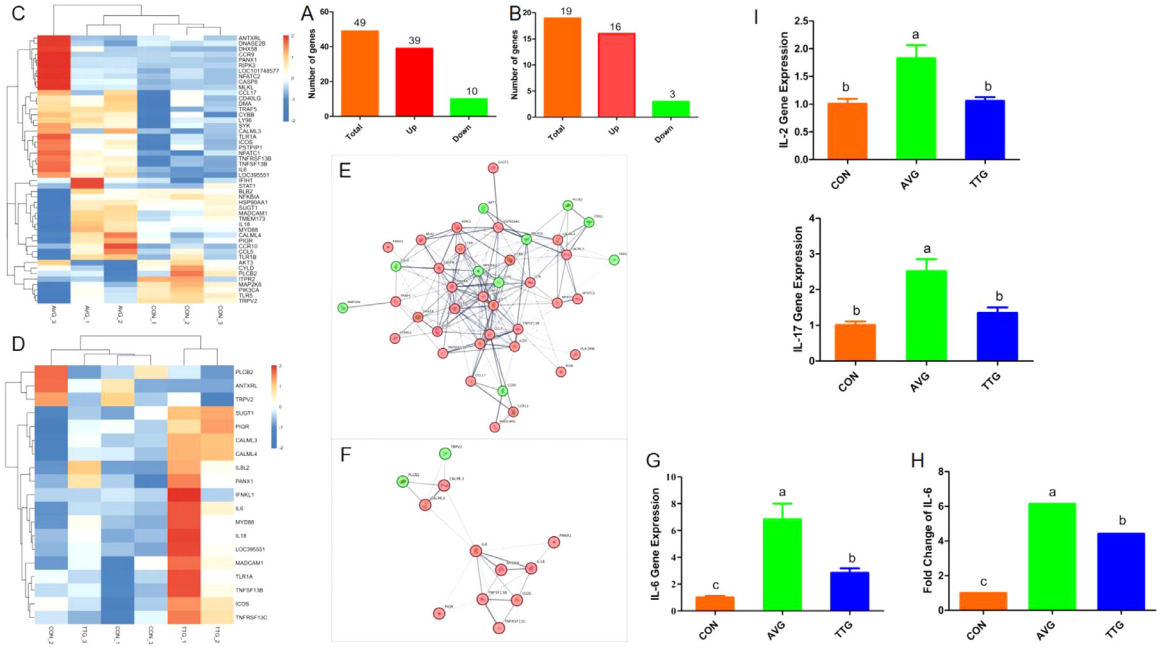

Figure 6. Chicken lung inflammation factor expression. (A) Immune gene number in the AVG. (B) Number of groups of immune genes in the TTG. (C) Immune genetic heat maps in the AVG. (D) Immune genetic heat maps in the TTG. (E) PPI analysis of the AVG. (F) PPI analysis of the TTG. (G) IL-6 mRNA expression. (H) IL-6 Fold Change. (I) Gene expression. CON: control group. AVG: H_2S-exposed group. TTG: TTO treatment group. Different letters between the groups indicate significant differences ($P < 0.05$). The data are expressed as mean ± standard deviation (M ± SD).

inflammatory response in chickens, the mRNA expression levels of cellular immune inflammation-related genes, such as NF-κB (nuclear factor kappa B), IL-17, and IL-2 were detected. After 42 d of H_2S exposure, the expression levels of IL-2 and IL-17 were significantly upregulated ($P < 0.05$). However, IL-2 and IL-17 mRNA expression levels in the chicken lungs of the TTG were significantly decreased ($P < 0.05$) and returned to more or less normal levels (Figure 6I). These results indicate that TTO has a favorable effect, alleviating the inflammatory response induced by H_2S.

Network Pharmacological Analysis

To further explore the specific effects of the TTO treatment on transcribed genes, we conducted a network pharmacological analysis of DEGs between the TTG and AVG. In this process, genes from the AVG and TTG were rigorously screened, selecting those with a FC > 1.2 and $P < 0.05$ as differential genes. After adhering to strict screening conditions, 762 significantly DEGs were identified, included 514 upregulated DEGs and 248 downregulated DEGs (Figure 7A). The Veen analysis of 93 drug targets and differential genes revealed 4 common targets (Figure 7B), thereby providing important insight into the mechanism of action of the TTO treatment at the transcriptional level. The GO analysis showed that the DEGs were mainly enriched in the plasma membrane, integral components of the membrane, cytoplasm, nucleus, cytosol, extracellular spaces, and integral components of plasma, extracellular region, metal ion binding, the way, such as ATP binding (Figure 7C). The KEGG analysis revealed significant alterations in DEGs involved in various pathways, including the P53 signaling pathway, ferroptosis, apoptosis, cell cycle, cellular senescence, necroptosis pathways, intestinal immune network for IgA production pathway, cytosolic DNA-sensing pathway, Toll-like receptor signaling pathway, NOD-like receptor signaling pathway and cytokine−cytokine receptor interaction pathway (Figure 7D). These results indicated that the TTO treatment could modify the effects of H_2S on cell death and immunity in chicken lungs.

The TCMSP database and Swiss Target Prediction yielded 93 key targets of active ingredients. Six active ingredients were identified in TTO, namely terpinen-4-ol, globulol, limonene, α-terpineol, terpinolene, and γ-Terpineol. The PPI analysis revealed that these 6 active ingredients acted on 4 targets: CA2 (carbonic anhydrase 2), CA4 (carbonic anhydrase 4), GABRA5 (gamma-aminobutyric acid type A receptor subunit alpha 5), and ADH1C (alcohol dehydrogenase 1C) (Figures 7E−7F), indicted that these were the main targets of the active components of TTO.

Molecular Docking

The 4 obtained targets (CA2, CA4, GABRA5, and ADH1C) were analyzed by molecular docking with the core components (terpinen-4-ol, globulol, limonene, α-terpineol, terpinolene and γ-Terpineol) (Figure 8). The active compounds showed good binding activity with all the targets (Figure 8A). Of note, binding affinity of less than -5.0 kcal/mol signifies good binding activity between the small molecule

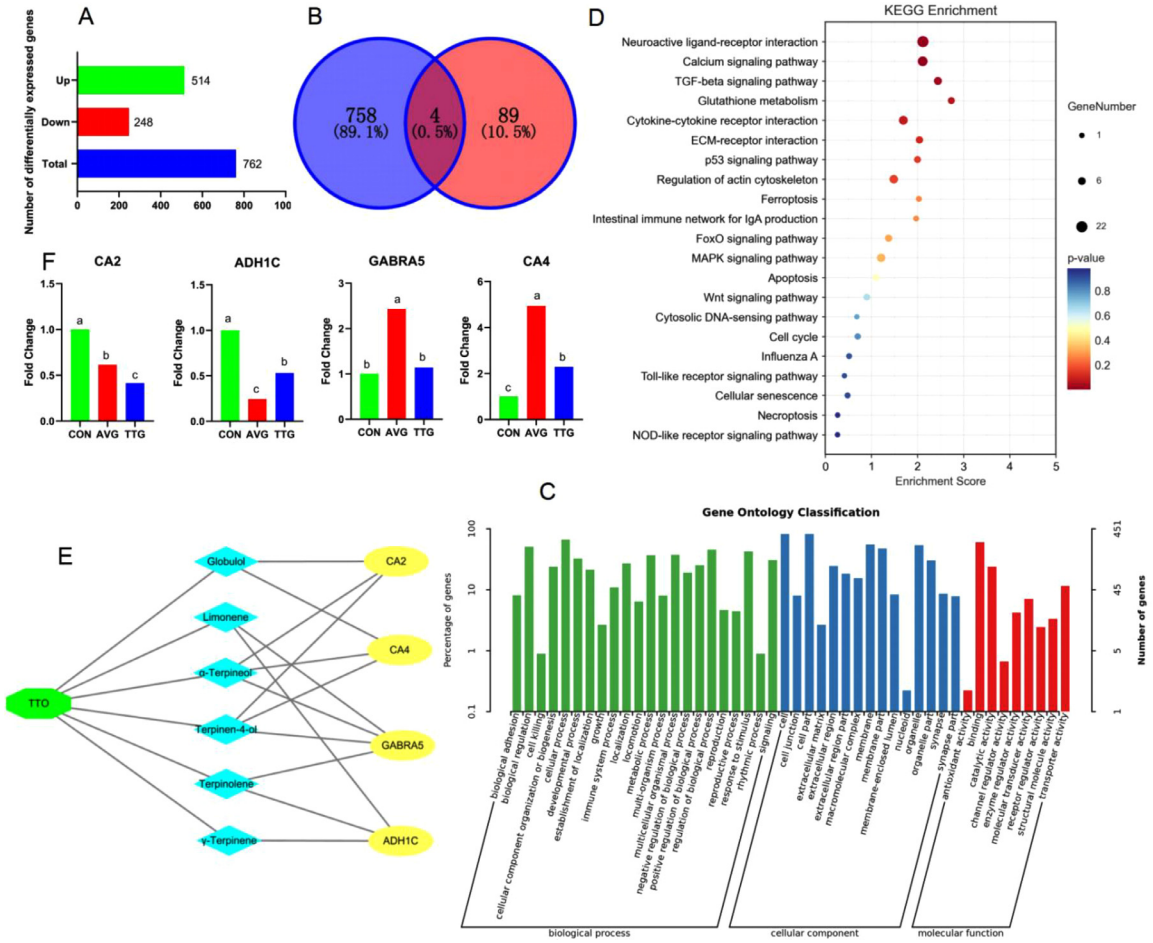

Figure 7. Transcriptome analysis of the different groups. (A) Differences in gene number. (B) Veen analysis. (C) GO enrichment analysis. (D) KEGG analysis. (E) TTO - pharmaceutical ingredients - target analysis. (F) Target gene FC trends. CON: control group. AVG: H_2S-exposed group. TTG: TTO treatment group. Different letters between the groups indicate significant differences ($P < 0.05$). The data are expressed as mean ± standard deviation (M ± SD).

ligand and the receptor protein, whereas binding affinity of less than -7.0 kcal/mol indicates even stronger binding activity. Among the tested compounds, the binding affinity of terpinen-4-ol with CA2 and CA4 was less than -5.0 kcal/mol (Figures 8C−8D). Similarly, the binding affinity of α-terpineol was less than -5.0 kcal/mol with CA4 (Figure 8N). Limonene exhibited a strong binding affinity of less than -5.0 kcal/mol with ADH1C (Figure 8K). Globulol also displayed a binding affinity of less than -5.0 kcal/mol with both CA2 and CA4 (Figures 8H, 8F). The binding affinity of terpinolene with GABRA5 and ADH1C was less than -5.0 kcal/mol (Figures 8I−8J). These findings suggest that the active components in TTO could be crucial mediators of its therapeutic effects in lung injury and that ADH1C, CA2, CA4 and GABRA5 might be the primary targets in H_2S-induced lung injury.

DISCUSSION

H_2S has been found to not only contribute to environmental pollution, but also harm organisms (Song et al., 2021). Specifically, studies have shown that H_2S causes significant damage to the respiratory system (Quist and Johnston, 2024). In poultry, exposure to H_2S has been observed to induce inflammation, oxidative stress, and apoptosis (Chi et al., 2018; Guo et al., 2019). Long-term exposure to environments rich in H_2S pollution has been identified as a serious threat to animal health (Wang et al., 2011; Zheng et al., 2019). TTO has attracted much attention for its properties of enhancing immunity and improved growth conditions in animals. However, the specific mechanism of how the active ingredients in tea tree oil treat H_2S-induced growth inhibition and lung oxidative stress still needs to be further explored and studied.

In recent years, studies on TTO have have demonstrated its ability to increase ADFI, ADG, and enhance feed conversion efficiency (Liu et al., 2023b). In this study, exposure to H_2S was observed to significantly reduce chicken body weight, F/G, ADFI, and ADG. However, chickens treated with TTO exhibited an increase in body weight, F/G, ADFI, and ADG. This improvement is primarily attributed to TTO's capacity to increase villus height and decrease crypt depth, thereby facilitating intestinal transport and absorption of amino acids and glucose (Wang et al., 2021b). Simultaneously, TTO has been found to increase the

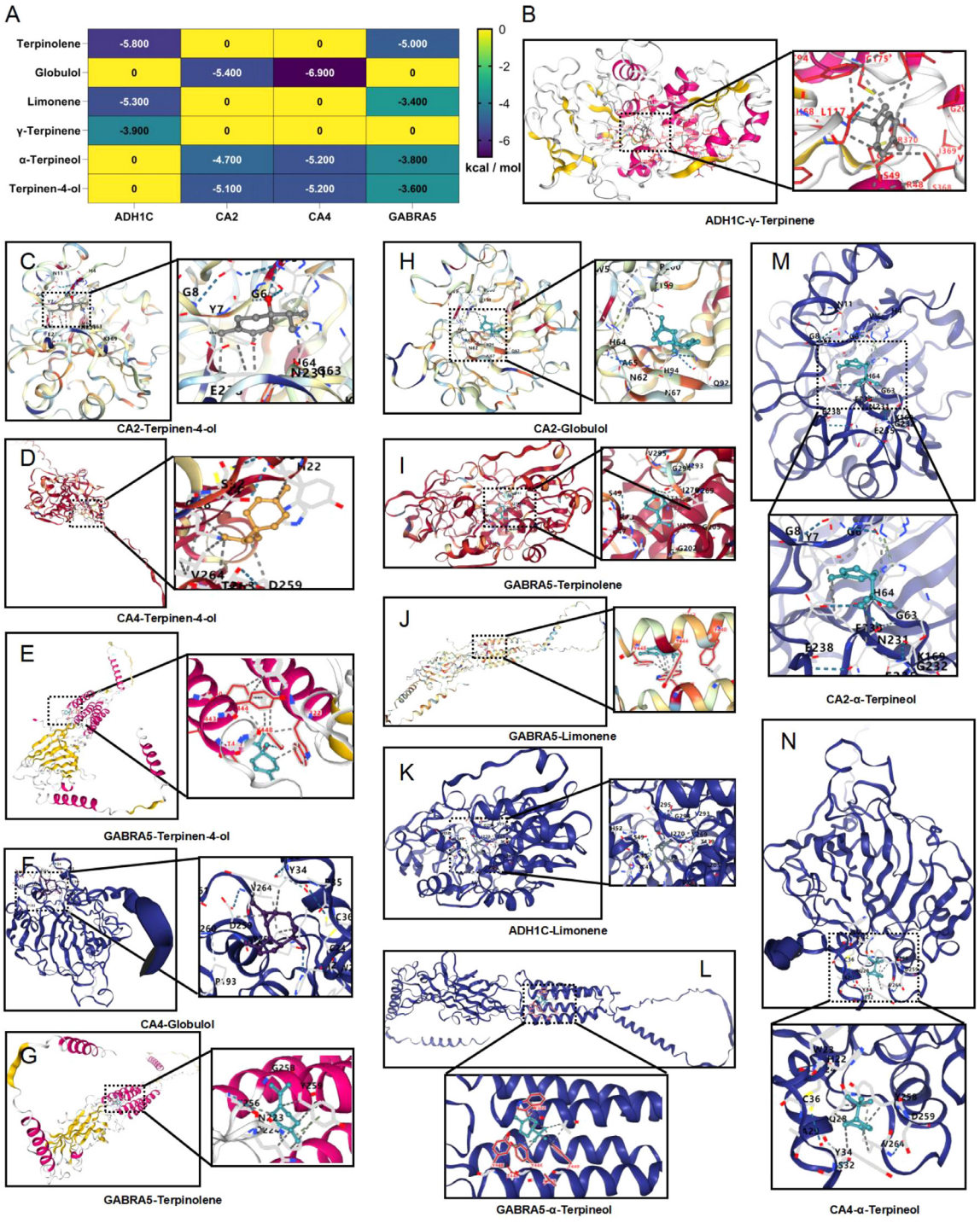

Figure 8. Molecular docking results of core targets and core components. (A) Heat map of binding affinity. (B) ADH1-γ-terpinene docking model. (C) CA2-terpinen-4-ol docking model. (D) CA4-terpinen-4-ol docking model. (E) GABRA5-terpinen-4-ol docking model. (F) CA4-globulol docking model. (G) GABRA5-terpinolene docking model. (H) CA2-globulol docking model. (I) GABRA5-terpinolene docking model. (J) GABRA5-limonene docking model. (K) ADH1-limonene docking model. (L) GABRA5-terpinolene docking model. (M) CA2-α-terpineol docking model. (N) CA4-α-terpineol docking model.

abundance of *Bacteroidetes* flora in the gut, facilitating the decomposition of polysaccharides and promoting fat deposition in the intestine (Shunan, 2017). In addition, the unique aromatic smell of TTO can stimulate the animal's appetite. The active ingredients in TTO can also enhance the activity of digestive enzymes after entering the digestive tract (Blachier et al., 2021). Furthermore, TTO promotes the digestion and absorption of nutrients in chickens, ultimately leading to increased ADFI, ADG, and improved feed conversion efficiency (Shunan, 2017). Similar findings have been made in previous studies that added tea tree oil to the drinking water of broilers significantly improved their intake and promoted their growth, a result consistent with this study (Running et al., 2019). In general, tea tree oil has a certain effect on alleviating the inhibitory effect of hydrogen sulfide on the growth performance of chickens.

H_2S-induced lung damage can trigger an oxidative stress response, a common physiological reaction in many organisms (Noctor et al., 2016). When H_2S stimulates chicken lungs, a large number of ROS are produced (Hu et al., 2018), which attack cell membrane proteins and DNA and induce apoptosis. Previous studies found that large amounts of ROS can cause lung tissue damage and hemorrhage (Liang et al., 2024). In this study, the TTO treatment significantly ameliorated H_2S-induced pulmonary hemorrhage. Apoptosis, also known as programmed cell death, is a spontaneous and orderly cell death process controlled by genes in order to maintain the body's normal metabolism. Generally, ROS produced in the body can trigger apoptosis (Liang et al., 2024). In this study, flow cytometry was to visually observe the impact of the TTO treatment on H_2S-induced apoptosis, including its effect on membrane potential, number of apoptotic cells, and ROS content. The results showed that H_2S significantly induced apoptosis, coincident with augmented ROS production and mitochondrial transmembrane potential depolarization. The TTO treatment effectively mitigated the apoptotic effects induced by H_2S, specifically by decreasing ROS levels and stabilized mitochondrial transmembrane potential. This indicates that TTO has the capability to suppress the mitochondrial apoptotic pathway. The transcriptome analysis in this study identified 28 DEGs related to cell apoptosis in the AVG, which is significantly higher than the eight apoptosis-related genes detected in the TTG. This suggests that TTO plays a substantial role in modulating the apoptotic pathway. The transcription results revealed significant expression of key apoptosis-related genes, included BID, Caspasa-6, Caspasa-8, and BCL2A1. The mRNA expression levels of Caspesa-9, BAK-1, BCL-2, and BAX genes were detected by qRT-PCR. The BCL-2 family can cause antiapoptotic gene BCL-2 expression and promote apoptosis gene BAX disorders, which can lead to mitochondrial apoptosis (Liang et al., 2024). In this study, the BCL2A1 gene inhibited BCL-2 gene expression, broke the balance between BAX and BCL-2, led to changes in the permeability of the cell membrane, the release of cytochrome, and further activation of Caspase-9 and Caspase-3 genes, thereby caused apoptosis (Liang et al., 2024). Previous studies have demonstrated that H_2S can activate the expression of BAX and BCL-2 genes by induced the generation of ROS in cells, which eventually led to mitochondrial damage and apoptosis (Liang et al., 2024). However, in the present study, the TTO treatment significantly decreased the mRNA expression of the BAK-1, BAX, and Caspesa-9 genes and increased the mRNA expression of the BCL-2 gene. This suggests that TTO has the potential to suppress apoptosis by modulating the mRNA expression of BCL-2, BAK-1, BAX, and Caspase-9. This is mainly due to the fact that the active ingredient terpinen-4-ol in TTO can increase the contents of SOD, CAT and other oxidases in the body, and thus realize the role of clearing ROS (Liu et al., 2023b). In addition, studies have also found that TTO can inhibit the activity of CYP1B1 enzyme and reduce lung damage caused by the activation of CYP450S/ROS pathway by H_2S (Liang et al.2024).

The TTO treatment effectively suppressed the inflammatory response induced by H_2S. In the process of inflammation, proinflammatory cytokines, such as IL-18, IL-6, and IL-17, play a pivotal role. The TTO treatment significantly reduced H_2S-induced the mRNA expression of inflammatory cytokines IL-2, IL-6, and IL-17, as detected by qRT-PCR. Thus, TTO can be used to reduce inflammation. IL-2 plays a role in immune cell proliferation, prevented excessive immune responsed that led to body damage. Previous studies have revealed that TTO can enhance serum levels of IFN-γ, TNF-α, and IL-2 (Liu et al., 2023b), thereby enhancing the body's immune function. All this may be attributed to the immunological regulation of terpinen-4-ol in TTO (Liu et al., 2023b).

In addition, IL-6, Myd88 and IL-18 were identified as key genes of TTO action based on the transcriptome sequencing data. IL-6 and IL-18, as important inflammatory factors, play important roles in caused inflammatory damage in the body (Cavalcanti et al., 2016). High expression of IL-18 can also inhibit humoral immunity (Kimata et al., 1992). The Myd88 gene, as a key gene in the TLR4/Myd88/NF-κB signaling pathway, plays an important role in regulated inflammatory factors (Chen et al., 2019). Previous research, TLR4/Myd88/NF-κB and high Myd88 gene expression can cause NF-κB signaling pathway activation. This, in turn, initiates the released of numerous inflammatory factors, included TNF-α, IL-6, and IL-18 (Pereira et al., 2022). Previous studies have also shown that TTO can significantly downregulate the expression of TLR4 and MyD88 genes (Chenglong, 2023). In this study, TTO significantly reduced the expression of MyD88 (FC = 1.86) induced by H_2S. Although TTO reduced the expression of MyD88 (FC = 1.56), it did not fully recover to a normal level. In addition, TTO has been found to significantly reduced IL-18 production in intestinal inflammation in the small intestine of pigs (Jun, 2022). In human studies, TTO has been shown to effectively inhibit the production of IL-1β and IL-6 by macrophages, mainly due to the terpinen-4-ol and α-terpineol components in TTO, which could inhibited the production of inflammatory factors (Nogueira et al., 2014). Consistent with these findings, in the present study, TTO significantly reduced the expression of IL-6.

To further explore the specific effects of TTO on related genes, this study focused on the main active ingredients of TTO (terpinen-4-ol, globulol, limonene, γ-terpineol, terpinolene, and α-terpineol). Through target prediction and analysis of these active components, 4 important core targets (CA2, CA4, GABRA5, and ADH1C) were found in 762 significant DEGs, suggesting that these targets may be important sites of action for the active components of TTO. Carbonic anhydrase (**CA**) is a functionally defined enzyme found mainly in red blood cells that catalyzes the conversion of carbon dioxide to bicarbonate and protons (Worden et al. 2009). Carbonic anhydrase plays an important role in

multiple physiological processes, such as gas transport, acid-base balance regulation, bone resorption and calcification, and ion transport (Worden et al. 2009). Of note, CA has an important function in eggshell formation, transporting large amounts of Ca^{2+} and CO_3^{2-} that are eventually deposited on eggs in the form of calcium carbonate (Tomita et al., 2011). Previous animal studies found that CA2 has 2 sulfhydryl groups, which may allow it to scavenge oxygen free radicals and thereby protect cells from oxidative damage (Zimmerman et al., 2008). It has also been found that lung calcification and fibrosis are closely related to the expression of the CA4 gene (Nava et al., 2022). GABRA5 plays an important role in the glucose balance and has an impact on body growth and development (Pei et al., 2022). In cattle studies, the ADH1C gene was found to affect muscle development and vitamin A metabolism (Jin et al., 2022). The results obtained in the current study demonstrate that TTO significantly modulates the expression of CA2, CA4, GABRA5, and ADH1C, further corroborating TTO's antioxidant properties and its potential to enhance growth performance. The altered expression of CA2, CA4, GABRA5, and ADH1C observed in this study may be attributed to ROS influencing gene transcription. The molecular docking analysis in this study revealed strong binding affinities between the active ingredients of TTO (terpinen-4-ol, globulol, limonene, α-terpineol, terpinolene, and γ-terpineol) and the targets CA2, CA4, GABRA5, and ADH1C. This study provides valuable new insights into the mechanism of action of TTO.

CONCLUSIONS

This study revealed that adding proper TTO to chick drinking water can significantly reduce the lung tissue damage caused by H_2S. Network pharmacology and transcriptomics analysis revealed that 6 active ingredients of TTO (terpinen-4-ol, globulol, limonene, α-terpineol, terpinolene, and γ-terpineol) primarily target 4 core proteins (CA2, CA4, GABRA5, and ADH1C) to ameliorate lung injury. These findings not only offer an effective solution for issues arising in the modernization of livestock and poultry production but also enrich the research content of TTO in the field of network pharmacology, providing novel perspectives and ideas for its future application and development.

ACKNOWLEDGMENTS

Thanks to the support of the National Defense Basic Research Program (16ZG6103).

Author Contributions: Yilei Liang: Conceptualization, Data curation, Writing—review and editing. Li Jiang: Formal analysis, Data curation, Investigation. Xuegang Luo: Supervision, Funding acquisition. Tingting Cheng: Methodology. Yachao Wang: Investigation, Writing—review and editing. Xiaoyan Long: Methodology.

DISCLOSURES

The authors declare no conflicts of interest.

SUPPLEMENTARY MATERIALS

Supplementary material associated with this article can be found in the online version at doi:10.1016/j.psj.2024.104180.

REFERENCES

Bekhof, A. S. M. W., F. P. A. M. van Hunsel, S. Koppel, and H. J. Woerdenbag. 2023. Safety assessment and adverse drug reaction reporting of tea tree oil (*Melaleuca aetheroleum*). Phytother. Res 37:1309–1318.

Blachier, F., M. Andriamihaja, P. Larraufie, E. Ahn, A. Lan, and E. Kim. 2021. Production of hydrogen sulfide by the intestinal microbiota and epithelial cells and consequences for the colonic and rectal mucosa. Am. J. Physiol-Gastr. L 320:125–135.

Bo, R. N., Y. W. Zhan, S. M. Wei, S. Y. Xu, Y. M. Huang, M. J. Liu, and J. G. Li. 2023. Tea tree oil nanoliposomes: optimization, characterization, and antibacterial activity against *Escherichia coli* in vitro and in vivo. Poult. Sci 102:102238.

Brings, C., J. Fröbel, P. Cadeddu, U. Germing, R. Haas, and N. Gattermann. 2022. Impaired formation of neutrophil extracellular traps in patients with MDS. Blood Adv 6:129–137.

Cavalcanti, N. G., C. D. Marque, E. Lins, T. U. Lins, M. C. Pereira, M. J. Rêgo, A. L. Duarte, R. Pitta. Ida, and M. G. Pitta. 2016. Cytokine profile in gout: inflammation driven by IL-6 and IL-18? Immunol. Invest 45:383–395.

Chen, M., X. Li, Q. Shi, Z. Zhang, and S. Xu. 2019. Hydrogen sulfide exposure triggers chicken trachea inflammatory injury through oxidative stress-mediated FOS/IL8 signaling. J Hazard Mater 368:243–254.

Chenglong, Y. 2023. The therapeutic effects of tea tree oil nanemulsion combined with caffeic acid against *Escherichia coliinduced* mastitis in rats. Yangzhou Univ 1:1–96.

Chi, Q., X. Chi, X. Hu, S. Wang, H. Zhang, and S. Li. 2018. The effects of atmospheric hydrogen sulfide on peripheral blood lymphocytes of chickens: perspectives on inflammation, oxidative stress and energy metabolism. Environ. Res 167:1–6.

Cully, M. 2014. Public health: the politics of antibiotics. Nature 1:7498–7509.

Groß, R., H. Reßin, P. von. Maltitz, D. Albers, L. Schneider, H. Bley, M. Hoffmann, M. Cortese, D. Gupta, M. Deniz, J. Y. Choi, J. Jansen, C. Preußer, K. Seehafer, S. Pöhlmann, D. R. Voelker, C. Goffinet, E. Pogge-von. Strandmann, U. Bunz, R. Bartenschlager, S. El. Andaloussi, K. M. J. Sparrer, E. Herker, S. Becker, F. Kirchhof.f, J. Münch, and J. A. Müller. 2024. Phosphatidylserine-exposing extracellular vesicles in body fluids are an innate defence against apoptotic mimicry viral pathogens. Nat. Microbiol 9:905–921.

Guo, J., H. Xing, M. Chen, W. Wang, H. Zhang, and S. Xu. 2019. H_2S inhalation-induced energy metabolism disturbance is involved in LPS mediated hepatocyte apoptosis through mitochondrial pathway. Sci. Total Environ. 663:380.

Hu, X., Q. Chi, D. Wang, X. Chi, X. Teng, and S. Li. 2018. Hydrogen sulfide inhalation-induced immune damage is involved in oxidative stress, inflammation, apoptosis and the Th1/Th2 imbalance in broiler bursa of fabricius. Ecotoxicol. Environ. Saf 164:201–209.

Huang, C.-B., L. Xiao, S.-C. Xing, J.-Y. Chen, Y.-W. Yang, Y. Zhou, W. Chen, J.-B. Liang, J.-D. Mi, Y. Wang, Y.-B. Wu, and X.-D. Liao. 2019. The microbiota structure in the cecum of laying hens contributes to dissimilar H_2S production. BMC Genomics 20:770.

Huang, P., P. Wang, J. X. Xu, M. S. Sun, X. B. Liu, Q. Lin, W. Liu, Z. X. Qing, and J. G. Zeng. 2021. Fermented traditional Chinese

medicine alters the intestinal microbiota composition of broiler chickens. Res. Vet. Sci 135:8–14.
Jin, X. C., D. Q. Peng, S. J. Kim, N. Y. Kim, J. G. Nejad, D. Kim, S. B. Smith, and H. G. Lee. 2022. Vitamin A supplementation downregulates ADH1C and ALDH1A1 mRNA expression in weaned beef calves. Anim. Nutr 10:372–381.
Jun, L. 2022. The regulatory effects of tea tree oil extract terpinen-4-ol LPS-induced intestinal injury in weaned piglets. Yangzhou Univ 1:1–76.
Khalaji, S., M. Zaghari, K. Hatami, S. Hedari-Dastjerdi, L. Lotfi, and H. Nazarian. 2012. Black cumin seeds, Artemisia leaves (*Artemisia sieberi*), and *Camellia L.* plant extract as phytogenic products in broiler diets and their effects on performance, blood constituents, immunity, and cecal microbial population. Poult. Sci 90:2500–2510.
Kimata H., A. Yoshida, C. Ishioka, I. Lindley, H. Mikawa, 1992. Interleukin 8 (IL-8) selectively inhibits immunoglobulin E production induced by IL-4 in human B cells. J Exp Med. 176:1227-1231
Li, H. H., S. Liu, L. C. Chen, J. Luo, D. Q. Zeng, and X. S. Li. 2021. Juvenile hormone and transcriptional changes in honey bee worker larvae when exposed to sublethal concentrations of thiamethoxam. Ecotoxicol. Environ. Saf 225:112744.
Li, X., M. Chen, Q. Shi, H. Zhang, and S. Xu. 2020. Hydrogen sulfide exposure induces apoptosis and necroptosis through lncRNA3037/miR-15a/BCL2-A20 signaling in broiler trachea. Sci. Total Environ. 699:134296.
Liang, Y., L. Jiang, M. Hu, X. Luo, T. Cheng, and Y. Wang. 2024. Tea tree oil inhibits hydrogen sulfide-induced oxidative damage in chicken lungs through CYP450s/ROS pathway. Poult. Sci 103:103860.
Liu, M., X. Xu, C. Sun, X. Zheng, Q. Zhou, C. Song, P. Xu, Q. Gao, and B. Liu. 2023a. Tea tree oil improves energy metabolism, nonspecific immunity, and microbiota diversity via the Intestine −hepatopancreas axis in *Macrobrachium* rosenbergii under low fish meal diet administration. Antioxidants 12:1879.
Liu, M., X. Zheng, C. Sun, Q. Zhou, B. Liu, and P. Xu. 2022. Tea tree oil mediates antioxidant factors relish and Nrf2-autophagy axis regulating the lipid metabolism of *Macrobrachium* rosenbergii. Antioxidants 11:2260.
Liu, Q., Y. L. Liu, X. F. Guan, J. H. Wu, Z. Q. He, J. N. Kang, Z. W. Tao, and Y. L. Deng. 2019. Effect of M2 macrophages on injury and apoptosis of renal tubular epithelial cells induced by calcium oxalate crystals. Kidney Blood Press Res 44:777–791.
Liu, Y., L. Xu, H. Du, J. Feng, W. Zhang, H. Li, F. Xu, J. Lin, H. Fu, X. Zhao, Y. Zheng, L.-J. Chang, and G. Shu. 2023b. Effects of adding tea tree oil on growth performance, immune function, and intestinal function of broilers. Poult. Sci 102:102936.
Lyublinskaya, O. G., J. S. Ivanova, N. A. Pugovkina, I. V. Kozhukharova, Z. V. Kovaleva, A. N. Shatrova, N. D. Aksenov, V. V. Zenin, Y. A. Kaulin, I. A. Gamaley, and N. N. Nikolsky. 2017. Redox environment in stem and differentiated cells: a quantitative approach. Redox Biol 12:758–769.
Nava, V. E., R. Khosla, S. Shin, F. E. Mordini, and B. C. Bandyopadhyay. 2022. Enhanced carbonic anhydrase expression with calcification and fibrosis in bronchial cartilage during COPD. Acta Histochemica 124:151834.
Noctor, G., A. Mhamdi, and C. H. Foyer. 2016. Oxidative stress and antioxidative systems: recipes for successful data collection and interpretation. Plant Cell Environ 39:1140–1160.
Nogueira, M. N. M., S. G. Aquino, C. Rossa Junior, and D. M. P. Spolidorio. 2014. Terpinen-4-ol and alpha-terpineol (tea tree oil components) inhibit the production of IL-1β, IL-6 and IL-10 on human macrophages. Inflammation Res 63:769–778.
Ortega, S., H. Fabelo, R. Camacho, M. D. Plaza, G. M. Callicó, and R. Sarmiento. 2018. Detecting brain tumor in pathological slides using hyperspectral imaging. Biomed. Opt. Express 9:818–831.
Pei, Z., Y. He, J. C. Bean, Y. Yang, H. Liu, M. Yu, K. Yu, I. Hyseni, X. Cai, H. Liu, N. Qu, L. Tu, K. M. Conde, M. Wang, Y. Li, N. Yin, N. Zhang, J. Han, C. H. S. Potts, N. A. Scarcelli, Z. Yan, P. Xu, Q. Wu, Y. He, Y. Xu, and C. Wang. 2022. Gabra5 plays a sexually dimorphic role in POMC neuron activity and glucose balance. Front. Endocrinol 13:889122.
Pereira, M., D. F. Durso, C. E. Bryant, E. A. Kurt-Jones, N. Silverman, D. T. Golenbock, and R. T. Gazzinelli. 2022. The IRAK4 scaffold integrates TLR4-driven TRIF and MYD88 signaling pathways. Cell Rep 40:111225.
Quist, A. J. L., and J. E. Johnston. 2024. Respiratory and nervous system effects of a hydrogen sulfide crisis in carson. California. Sci. Total Environ. 906:167480.
Ruan, D., Q. L. Fan, S. Zhang, H. K. EI-Senousey, A. M. Fouadt, X. J. Lin, X. L. Dong, Y. F. Deng, S. J. Yan, C. T. Zheng, Z. Y. Jiang, and S. Q. Jiang. 2023. Dietary isoleucine supplementation enhances growth performance, modulates the expression of genes related to amino acid transporters and protein metabolism, and gut microbiota in yellow-feathered chickens. Poult. Sci 102:102774.
Running, W., P. Jia-giang, Z. M-q, Q. N. L.Y, H. L. m, and X. Z. 2019. Effects of *Melaleuca alterniflora* oil (tea tree oil) on intestinal mucosal tissue structureand intestinal immune cells in broilers. Ch.J Vet. Sci. 4:751–755.
Shi, X., T. Xu, M. Gao, Y. Bi, J. Wang, Y. Yin, and S. Xu. 2024. Combined exposure of emamectin benzoate and microplastics induces tight junction disorder, immune disorder and inflammation in carp midgut via lysosome/ROS/ferroptosis pathway. Water Research 257:121660.
Shunan, W. 2017. Effects of tea tree oil on growth performance andIntestinal barrier function of weaned piglets. Yangzhou Univ 1:1–79.
Song, N., W. Wang, Y. Wang, Y. Guan, S. Xu, and M. Y. Guo. 2021. Hydrogen sulfide of air induces macrophage extracellular traps to aggravate inflammatory injury via the regulation of miR-15b-5p on MAPK and insulin signals in trachea of chickens. Sci. Total Environ 771:145407.
Sun, W., Y. Lei, Z. Jiang, K. Wang, H. Liu, and T. Xu. 2024. BPA and low-Se exacerbate apoptosis and mitophagy in chicken pancreatic cells by regulating the PTEN/PI3K/AKT/mTOR pathway. J. Adv. Res. 1232:32–41.
Szymański, A., and A. Rossa. 2020. The modified fuzzy mortality model based on the algebra of ordered fuzzy numbers. Biom J 63:671–689.
Tian, Q., and X. Piao. 2019. Essential oil blend could decrease diarrhea prevalence by improving antioxidative capability for weaned pigs. Animals 9:847.
Tomita, Y., T. I, N. I, K. O, and K. A. 2011. Biochemical and developmental characterization of carbonic anhydrase II from chicken erythrocytes. Acta Vet Scand 53:16–24.
Wang, L. X., Y. Zhang, L. Liu, F. Huang, and B. Dong. 2021b. Effects of three-layer encapsulated tea tree oil on growth performance, antioxidant capacity, and intestinal microbiota of weaned pigs. Front. Vet. Sci 8:789225.
Wang, Y., M. Huang, Q. Meng, and Y. Wang. 2011. Effects of atmospheric hydrogen sulfide concentration on growth and meat quality in broiler chickens. Poult. Sci 90:2409.
Worden, A. Z., J. H. Lee, T. Mock, P. Rouzé, M. P. Simmons, A. L. Aerts, A. E. Allen, M. L. Cuvelier, E. Derelle, M. V. Everett, E. Foulon, J. Grimwood, H. Gundlach, B. Henrissat, C. Napoli, S. M. McDonald, M. S. Parker, S. Rombauts, A. Salamov, V. D. P, J. H. Badger, P. M. Coutinho, E. Demir, I. Dubchak, C. Gentemann, W. Eikrem, J. E. Gready, U. John, W. Lanier, E. A. Lindquist, S. Lucas, K. F. Mayer, H. Moreau, F. Not, R. Otillar, O. Panaud, J. Pangilinan, I. Paulsen, B. Piegu, A. Poliakov, S. Robbens, J. Schmutz, E. Toulza, T. Wyss, A. Zelensky, K. Zhou, E. V. Armbrust, D. Bhattacharya, U. W. Goodenough, V. Peer, and V. Grigoriev. 2009. Green evolution and dynamic adaptations revealed by genomes of the marine picoeukaryotes micromonas. Science 324:268–272.
Yang, T. Y., F. Feng, K. Zhan, X. Y. Ma, M. C. Jiang, O. Datsomor, X. Y. Zhu, Y. J. Huo, and G. Q. Zhao. 2022. Effect of the tea tree oil on growth performance, meat quality, serum biochemical indices, and antioxidant capacity in finishing pigs. Front. Vet. Sci 9:916625.
Zheng, S., X. Jin, M. Chen, Q. Shi, H. Zhang, and S. Xu. 2019. Hydrogen sulfide exposure induces jejunum injury via CYP450s/ROS pathway in broilers. Chemosphere 214:25.
Zimmerman, U. J. P., P. Wang, X. Zhang, S. Bogdanovich, and R. E. Forster. 2008. Anti-oxidative response of carbonic anhydrase III in skeletal muscle. IUBMB Life 56:343–347.